First-Principles Evaluation of Dynamical Response and Plasmon Dispersion in Metals

Andrew A. Quong

Complex Systems Theory Branch, Code 6690, Naval Research Laboratory, Washington, D.C. 20375-5345

Adolfo G. Eguiluz[(a)]

Fritz-Haber-Institut der Max-Planck-Gesellschaft, Faradayweg 4-6, 1000 Berlin 33, Germany

(Received 21 December 1992)

We report an *ab initio* evaluation of the dynamical density-response function for *real* Al and Na. The method we employ is a generalization of the Dalgarno-Lewis scheme of perturbation theory to systems with a continuous spectrum and to dynamical problems. The crystal lattice is found to lower the plasmon frequency of Al for large wave vectors by as much as 4 eV. For this metal, agreement with experiment is excellent in the time-dependent local-density approximation for exchange correlation. The "anomalous" dispersion observed for Na for large wave vectors is assigned to subtler exchange-correlation effects.

PACS numbers: 71.45.Gm, 71.10.+x, 72.30.+q

The dynamical density-response function $\chi(\mathbf{x},\mathbf{x}'|\omega)$ plays a fundamental role in the theoretical study of the metallic state of matter [1]. This response function is directly related to observables—such as inelastic electron scattering cross sections and plasmon dispersion relations [1,2]—is a key building block in studies of quasiparticle excitations [2]; from its knowledge one can calculate the correlation contribution to the ground-state energy [2], etc.

However, progress in the actual computation of $\chi(\mathbf{x},\mathbf{x}'|\omega)$ for a real metal has been slow. Most available studies are based on the electron-gas model, in which one concentrates on the effects of the electron-electron interaction and ignores the effects of the crystal structure [1,2]. Perturbative schemes for the inclusion of the effects of the lattice have been developed in recent years [3,4]. Plasmon-pole approximations, whose physics is basically rooted in the electron-gas model, have also been proposed [5–7]. Only one *ab initio* calculation of the dynamical response of a real metal has been performed to date (for Ni) [8]—a few such calculations have been reported for bulk semiconductors [9–11].

In this Letter we report a first-principles evaluation of the dynamical density-response function of bulk Al and Na, performed—for the first time—with full inclusion of the effects of the crystal structure. The method we use is inspired by the Dalgarno-Lewis scheme of Rayleigh-Schrödinger perturbation theory [12] for the evaluation of sums over the energy spectrum of an atom. Our approach eliminates the need to carry out sums over the unoccupied bands [5–11], is formulated for dynamical response, and is designed to produce the full response function, not just the induced density. The last two features, which go beyond recently developed static-response methods [13–15], are a must for the study of many-body effects [2,16] and for making contact with various spectroscopies [2].

From the response function—which we evaluate in a plane-wave basis, with the use of *ab initio,* norm-conserving pseudopotentials [17]—we extract plasmon dispersion curves. We find the effect of the lattice to be particularly significant for the case of Al. The plasmon dispersion curve obtained for this metal in the time-dependent extension of local-density functional theory (TDLDA) [18] is in quantitative agreement with experiment [19]. In the case of Na, the residual disagreement between our crystal TDLDA results and experiment for small wave vectors is understood on physical grounds (core polarization). We attribute the "anomalous" dispersion observed experimentally for this alkali metal for large wave vectors [20] to exchange-correlation (XC) effects which are beyond the TDLDA.

The density-response function χ is related to the irreducible polarizability $\tilde{\chi}$ through the (formally exact) Bethe-Salpeter integral equation [1,2]

$$\chi(\mathbf{x},\mathbf{x}'|\omega)=\tilde{\chi}(\mathbf{x},\mathbf{x}'|\omega)+\int d^3x''\int d^3x'''\tilde{\chi}(\mathbf{x},\mathbf{x}''|\omega)v(\mathbf{x}'',\mathbf{x}''')\chi(\mathbf{x}''',\mathbf{x}'|\omega)\,, \tag{1}$$

where v is the bare Coulomb interaction. In the random-phase approximation (RPA) we set $\tilde{\chi}=\chi^0$, where χ^0 is the polarizability for noninteracting electrons. A simple way to go beyond the RPA, i.e., to include short-range correlations ("vertex corrections") in Eq. (1), is the TDLDA ansatz [18], in which $\tilde{\chi}=\chi^0$ and v is replaced by the effective interaction $V(\mathbf{x}-\mathbf{x}')=v(\mathbf{x}-\mathbf{x}')+dV_{\rm XC}(\mathbf{x})/dn(\mathbf{x})\delta(\mathbf{x}-\mathbf{x}')$, where $V_{\rm XC}(\mathbf{x})$ is the XC potential for the electron density $n(\mathbf{x})$. In what follows our notation refers explicitly to the RPA; the TDLDA is obtained simply by replacing v by V everywhere.

The polarizability χ^0 is defined in terms of the eigenvalues and eigenfunctions of an appropriate one-electron Hamiltonian $\hat{H}$ [21] by the equation

$$\chi^0(\mathbf{x},\mathbf{x}'|\omega)=\sum_{\lambda\lambda'}\frac{f_\lambda-f_{\lambda'}}{E_\lambda-E_{\lambda'}+\hbar(\omega+i\eta)}\times\phi_\lambda^*(\mathbf{x})\phi_{\lambda'}(\mathbf{x})\phi_{\lambda'}^*(\mathbf{x}')\phi_\lambda(\mathbf{x}')\,. \tag{2}$$

This standard representation for χ^0 [22] has tradition-

ally represented a numerical bottleneck in response calculations for crystals [5–11]. The sums over the unoccupied bands have been shown to converge slowly [23], and the additional sums over the Brillouin zone (BZ) are also slowly convergent. Furthermore, if the evaluation of χ^0 is to be based on a minimal-basis-set band structure, it would seem preferable to avoid explicit use of the unoccupied bands, since these may be poorly known.

We proceed in terms of the kernel $K(\mathbf{x},\mathbf{x}'|\omega)=\int d^3x''\times\chi(\mathbf{x},\mathbf{x}''|\omega)v(\mathbf{x}''-\mathbf{x}')$, typically encountered in linear-response and many-body studies [1,2,16]. We introduce an auxiliary function of the electron-position operator, $\Theta(\mathbf{x}_{\rm op},\mathbf{x}'|\omega)$, by the equation [12]

$$\langle\lambda'|\Theta(\mathbf{x}_{\rm op},\mathbf{x}'|\omega)|\lambda\rangle=\frac{\langle\lambda'|v(\mathbf{x}_{\rm op},\mathbf{x}')|\lambda\rangle}{E_\lambda-E_{\lambda'}+\hbar(\omega+i\eta)}\,, \tag{3}$$

designed to allow us to use in Eq. (2) the closure relation for the eigenkets of $\hat{H}$ [24]. We are thus led to the following representation for the noninteracting kernel $K^0=\chi^0 v$:

$$K^0(\mathbf{x},\mathbf{x}'|\omega)=\sum_\lambda f_\lambda\{\phi_\lambda^*(\mathbf{x})\psi_\lambda(\mathbf{x},\mathbf{x}'|\omega)+\phi_\lambda(\mathbf{x})\psi_\lambda^*(\mathbf{x},\mathbf{x}'|-\omega)\}\,, \tag{4}$$

where $\Psi_\lambda(\mathbf{x},\mathbf{x}'|\omega)\equiv\langle\mathbf{x}|\Theta(\mathbf{x}_{\rm op},\mathbf{x}'|\omega)|\lambda\rangle$, and the sum runs over the *occupied* states only.

The operator Θ is not obtained directly—rather the "polarizability wave functions" $\Psi_\lambda(\mathbf{x},\mathbf{x}'|\omega)$ are. From Eq. (3) these can be shown to satisfy an inhomogeneous partial differential equation,

$$\left[-\frac{\hbar^2}{2m}\nabla^2+V_{\rm sc}(\mathbf{x})-E_\lambda-z\right]\psi_\lambda(\mathbf{x},\mathbf{x}'|z)=v(\mathbf{x}-\mathbf{x}')\phi_\lambda(\mathbf{x})\,, \tag{5}$$

where the potential $V_{\rm sc}(\mathbf{x})$ *is known,* i.e., it is determined self-consistently with the wave functions $\{\phi_\lambda\}$ in the ground-state calculation. Thus the only unknown in Eq. (5) are the $\{\Psi_\lambda\}$ for the states which contribute to Eq. (4)—the *occupied* states. Equations (4) and (5), and the integral equation (1), or its counterpart $K=K^0+K^0K$, are the essence of our method.

Several linear-response methods [13–15,18,25] are encompassed by the above scheme [12], which is similar to Green's-function methods [18] which, however, have only been implemented for effective one-dimensional motion, such as atoms in the central-field approximation [13,18] and clusters treated within the jellium model [25]. Equation (5) is a finite-frequency, "nondiagonal" (i.e., it applies for all $\mathbf{x},\mathbf{x}'$ pairs), generalization [26] of the central equation in the "modified" Sternheimer method [13], developed originally for atoms, and applied to semiconductors by Baroni and co-workers [14] and Gonze and Vigneron [15].

Our algorithm provides the full *complex* response in one step, i.e., Eq. (5) is solved directly for a complex frequency $z=\omega+i\eta$ [27]. In the collisionless regime [1] $\eta=0^+$; in practice we give η a nonzero value. (In the present calculations $\eta=0.075$ Ry.) We emphasize that the structure of the operator Θ [24] ensures that $\mathrm{Im}\chi^0(\omega)\to 0$ for $\omega\to 0$, unlike response schemes which define $\mathrm{Im}\chi^0$ separately as a sum over broadened δ functions [8].

We have implemented the above formalism in a plane-wave basis, and applied it to bulk Al and Na. The ground-state properties were determined by solving the Kohn-Sham equation [21] in the local-density approximation, with use of *ab initio,* norm-conserving pseudopotentials [17]. In the case of Na there is appreciable overlap between the core and valence electron densities, which must be accounted for in the generation of the pseudopotential. This is achieved by carrying the atomic core electron density into the self-consistent calculation for the crystal [28]. The energy cutoff used was 12 Ry for Al and 8 Ry for Na. The sum over the BZ was performed on $20\times20\times20$ Monkhorst and Pack meshes [29], which correspond to 110 and 70 points in the irreducible element of the BZ for Al and Na, respectively [30]. The same numerical parameters were used in each case in Eq. (4) for the response calculations.

Every response quantity is expanded in a Fourier series, such as

$$\psi_\lambda(\mathbf{x},\mathbf{x}'|z)=\sum_{\mathbf{q}\mathbf{G}}\sum_{\mathbf{q}'\mathbf{G}'}b^\lambda_{\mathbf{G}\mathbf{G}'}(\mathbf{q},\mathbf{q}'|z)e^{i(\mathbf{q}+\mathbf{G})\cdot\mathbf{x}}e^{-i(\mathbf{q}'+\mathbf{G}')\cdot\mathbf{x}'}\,, \tag{6}$$

where $\mathbf{q}$ is a wave vector in the first BZ and $\mathbf{G}$ denotes a reciprocal lattice vector. Equation (5) is thus turned into a matrix equation of the form

$$\sum_{\mathbf{G}''}[H_{\mathbf{G}\mathbf{G}''}(\mathbf{q},\mathbf{q}|z)-\delta_{\mathbf{G}\mathbf{G}''}(E_\lambda-z)]b^\lambda_{\mathbf{G}''\mathbf{G}'}(\mathbf{q},\mathbf{q}'|z)=a^\lambda_{\mathbf{G}\mathbf{G}'}(\mathbf{q},\mathbf{q}')\,, \tag{7}$$

where $a^\lambda_{\mathbf{G}\mathbf{G}'}$ is the matrix of the Fourier coefficients of the right-hand side of Eq. (5). Equation (7) must be solved many times; after the first solution, which scales as N^3, subsequent solutions require $O(N^2)$ operations. For the present set of calculations the computer requirements amount to about 20 CPU sec on a Cray Y-MP supercomputer for each $(\mathbf{q},\omega)$ pair, a remarkably modest requirement compared with machine times quoted [6,31] for comparable-size problems attacked by other methods —several CPU hours.

The differential cross section for a process in which a (fast) electron is scattered by a crystal with energy transfer $\hbar\omega$ and momentum transfer $\hbar\mathbf{q}$ is proportional to $\mathrm{Im}\chi_{\mathbf{G}\mathbf{G}}(\mathbf{q}-\mathbf{G}|\omega)$ [1], where $\mathbf{G}$ is such that $\mathbf{q}-\mathbf{G}$ lies inside the first BZ. [A factor of $v^2(q)$ in the cross section strongly favors small momentum transfers.] In Fig. 1 we show this "loss function" for Al, for the range of wave vectors for which the plasmon has been observed via electron energy-loss spectroscopy (EELS) [19]. The dominant feature is the plasmon peak, whose qualitative behavior as a function of $(\mathbf{q},\omega)$ is easily visualized in terms of the f-sum rule (mathematically, the first moment of $\mathrm{Im}\chi$ grows as q^2 [1]; physically, charge conservation in the response process): the peak disperses upward in ener-

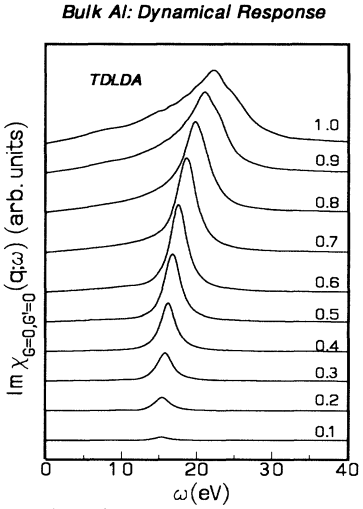

FIG. 1. Dynamical density response function for Al, calculated in the TDLDA. The family of curves shown is labeled by the magnitude of the wave vector transfer $\mathbf{q}=(q,0,0)$, given in units of $2\pi/a_0$, where a_0 is the lattice constant. (The largest q equals 1.55 Å^{-1}; we note that $k_F=1.75$ Å^{-1}.)

gy while damping out for large q's due to decay into electron-hole pairs. Indeed our response function fulfills this sum rule to very good accuracy, i.e., within a few percent for small q's, for which the width of Imχ is almost entirely numerical, and to better than 1% for larger q's. We view this result as a measure of the overall accuracy for our numerical calculations.

From the energy position of the peak in Im$\chi_{\mathbf{GG}}$ as a function of $\mathbf{q}$ we obtain the plasmon dispersion curves shown in Figs. 2 and 3 (for which the relevant $\mathbf{G}=0$). We consider the case of Al first. Figure 2(a) shows the results of three sets of RPA calculations, performed, respectively, for the electron gas (jellium model) and for two different plasmon propagation directions for the actual crystal. Figure 2(b) shows the RPA and TDLDA dispersion curves for the crystal. The position of the EELS loss [19] versus q is shown in both panels.

The key conclusions to be drawn from Fig. 2 are two: (i) *the effect of the lattice* on the plasmon dispersion curve for this "nearly-free-electron metal" *is in fact large,* amounting to $\sim$0.5 eV for $q\rightarrow 0$, and $\sim$4 eV for large q's, and (ii) *the TDLDA dispersion curve agrees extremely well with experiment for all wave vectors.* [Additionally, as illustrated by Fig. 2(a), we have that the plasmon energy does not depend on the direction of $\mathbf{q}$.] Both physical features, namely, the effect of the crystal structure and the many-body effect of the short-range correlations included in TDLDA are responsible for this agreement—*for Al, the crystal effect is the larger of the two.*

Note that a direct consequence of this result is that previous theoretical efforts [32] to explain the experimental plasmon dispersion curve for Al—a canonical example of electron-gas behavior—based on models which center

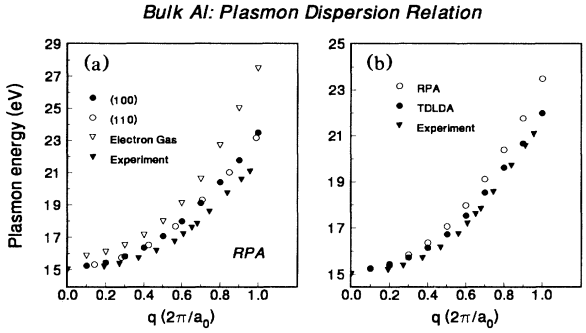

FIG. 2. Plasmon dispersion relations for Al—see text.

on the treatment of Coulomb correlations for electrons in jellium need to be reexamined.

A similar set of calculations was performed for Na. From Fig. 3(a) we have that the effect of the lattice is not as pronounced as it is for Al. For q's up to about 0.4 (in the units of the figure) the theoretical dispersion follows the EELS data [20] quite well. The relatively small quantitative discrepancy with experiment can be understood in terms of core-polarization effects which are not included in our pseudopotential calculations. On the other hand, while the inclusion of XC effects in TDLDA [Fig. 3(b)] again improves the agreement with experiment [20], the clear anomaly seen in the experimental data for large q's is not reproduced by the theory.

Since we have treated the effects of the lattice without approximation (except for the neglect of core polarization), we conclude that the behavior of the plasmon dispersion curve observed for Na for large q's must be due to XC effects which are outside the TDLDA. It is of interest to note that for the heavier alkalis the plasmon dispersion relation becomes increasingly anomalous [20], culminating with the so-called "RPA catastrophe" [33] for Cs. The study of such many-body effects remains a theoretical challenge.

In summary, on the basis of the evaluation of the dynamical density-response function and plasmon dispersion curves for real Al and Na we have shown that first-principles computations of dynamical properties of real metals are now feasible. The application of our method

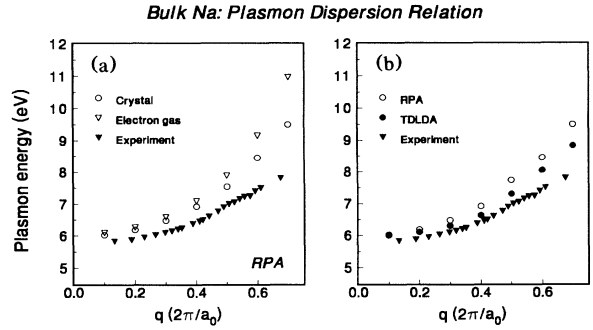

FIG. 3. Plasmon dispersion relations for Na—see text.

to *d*-electron metals is currently in progress.

We thank A. Fleszar for very useful discussions. A. A. Q. acknowledges support from the National Research Council and the Pittsburgh Supercomputer Center. A.G.E. acknowledges support from NSF Grant No. DMR-9207747, the San Diego Supercomputer Center, and Cray Research, Inc.

Note added.—A new set of measurements of the dynamical structure factor of Al has been published after completion of our work [34]. The theoretical interpretation of these measurements given in Ref. [34] is *entirely within the jellium model.* Interestingly, we have subsequently found that for the large wave vectors considered in Ref. [34] (they are much larger than the ones considered in the present paper) *band-structure effects* —which we have for the first time fully included in the evaluation of the dynamical density-response function —*account very well for the double-peak loss structure observed experimentally.* (See Fig. 2 of Ref. [34]; for the wave vector in question the plasmon mode discussed in the present paper has completely damped out.) Such effects will be discussed in detail in another publication.

[a]Permanent address: Department of Physics, Montana State University, Bozeman, MT 59717.

[1] D. Pines and P. Nozières, *The Theory of Quantum Liquids* (Benjamin, Reading, MA, 1964).

[2] G. D. Mahan, *Many-Particle Physics* (Plenum, New York, 1990), 2nd ed.

[3] K. Sturm and L. E. Oliveira, Phys. Rev. B **40**, 3672 (1989).

[4] M. Taut and K. Sturm, Solid State Commun. **82**, 295 (1992).

[5] M. S. Hybertsen and S. G. Louie, Phys. Rev. B **38**, 4033 (1988).

[6] W. von der Linden and P. Horsch, Phys. Rev. B **37**, 8351 (1988).

[7] G. E. Engel, B. Farid, C. M. M. Nex, and N. H. March, Phys. Rev. B **44**, 13356 (1991).

[8] F. Aryasetiawan, U. von Barth, P. Blaha, and K. Schwartz (to be published).

[9] W. Hanke and L. J. Sham, Phys. Rev. B **21**, 4656 (1980).

[10] L. R. W. Godby, M. Schlüter, and L. J. Sham, Phys. Rev. B **37**, 10159 (1988).

[11] R. Daling, W. van Haeringen, and B. Farid, Phys. Rev. B **44**, 2952 (1991).

[12] A. Dalgarno and J. T. Lewis, Proc. R. Soc. London A **233**, 70 (1955); see also E. Merzbacher, *Quantum Mechanics* (Wiley, New York, 1970), 2nd ed.

[13] G. D. Mahan and K. R. Subbaswamy, *Local Density Theory of Polarizability* (Plenum, New York, 1990).

[14] S. Baroni, P. Giannozzi, and A. Testa, Phys. Rev. Lett. **58**, 1861 (1987); P. Giannozzi, S. de Gironcoli, P. Pavone, and S. Baroni, Phys. Rev. B **43**, 7231 (1991).

[15] X. Gonze and J.-P. Vigneron, Phys. Rev. B **39**, 13210 (1989); A. Fleszar and X. Gonze, Phys. Rev. Lett. **64**, 2961 (1990).

[16] A. G. Eguiluz, M. Heinrichsmeier, A. Fleszar, and W. Hanke, Phys. Rev. Lett. **68**, 1359 (1992).

[17] N. Troullier and J. L. Martins, Phys. Rev. B **43**, 1993 (1991).

[18] A. Zangwill and P. Soven, Phys. Rev. A **21**, 1561 (1980); M. J. Stott and E. Zaremba, *ibid.* **21**, 12 (1980).

[19] E. Petri and A. Otto, Phys. Rev. Lett. **34**, 1283 (1975).

[20] A. vom Felde, J. Sprösser-Prou, and J. Fink, Phys. Rev. B **40**, 10181 (1989).

[21] W. Kohn and L. J. Sham, Phys. Rev. **140**, A1133 (1965).

[22] In Eq. (2) f_λ is a $T=0$ K Fermion occupation number. A smearing of about 20 mRy was used in performing BZ summations.

[23] M. S. Hybertsen and S. G. Louie, Phys. Rev. B **35**, 5585 (1987).

[24] The operator Θ is not Hermitian, i.e., $[\Theta(\mathbf{x}_{op},\mathbf{x}'|\omega)]^+ = -\Theta(\mathbf{x}_{op},\mathbf{x}'|-\omega)$. This condition ensures that $\mathrm{Re}\chi(\omega) = \mathrm{Re}\chi(-\omega)$ and $\mathrm{Im}\chi(\omega) = -\mathrm{Im}\chi(-\omega)$.

[25] J. M. Pacheco and W. Ekardt, Ann. Phys. (Leipzig) **1**, 255 (1992).

[26] In the method of Ref. [14] the potential on the right-hand side is the induced potential, and self-consistency is achieved by an iterative solution of that equation. In our method self-consistency is built into Eq. (1).

[27] Our method is particularly simple to implement on the imaginary-frequency axis, a useful feature for electron self-energy studies (Ref. [16]).

[28] S. G. Louie, S. Froyen, and M. L. Cohen, Phys. Rev. B **26**, 1738 (1982).

[29] H. J. Monkhorst and J. D. Pack, Phys. Rev. B **13**, 5188 (1976).

[30] For Al (Na) we obtain a lattice constant of 4.01 Å (4.10 Å), and a bulk modulus of 74 GPa (8.7 GPa). The corresponding experimental values (extrapolated to $T=0$ K) are 4.02 Å (4.21 Å) and 72 GPa (7.4 GPa). Gradient corrections to LDA have been shown to improve the agreement with experiment for Na—see J. P. Perdew *et al.*, Phys. Rev. B **46**, 6671 (1992). For the response calculations we have used the room-temperature value of the lattice constant (4.05 Å for Al, and 4.225 Å for Na).

[31] F. Bechstedt, Festkörperprobleme **32**, 161 (1992).

[32] R. G. Dandrea, N. W. Ashcroft, and A. E. Carlsson, Phys. Rev. B **34**, 2097 (1986).

[33] E. W. Plummer, G. M. Watson, and K.-D. Tsuei, in *Surface Science*, edited by M. Cardona and F. Ponce (Springer-Verlag, Berlin, 1991), p. 49.

[34] P. M. Platzman, E. D. Isaacs, H. Williams, P. Zschack, and G. E. Ice, Phys. Rev. B **46**, 12943 (1992).